Journal of Neurology (2022) 269:3841–3857
https://doi.org/10.1007/s00415-022-11021-1

ORIGINAL COMMUNICATION

The role of cerebellar damage in explaining disability and cognition in multiple sclerosis phenotypes: a multiparametric MRI study

Raffaello Bonacchi[1,2] · Alessandro Meani[1] · Elisabetta Pagani[1] · Olga Marchesi[1] · Massimo Filippi[1,2,3,4,5] · Maria A. Rocca[1,2,5]

Received: 24 November 2021 / Revised: 7 February 2022 / Accepted: 9 February 2022 / Published online: 1 March 2022

Abstract

Background Cerebellar involvement is not comprehensively studied from an MRI point of view in multiple sclerosis (MS). We aimed to quantify cerebellar damage and identify predictors of physical disability and cognitive dysfunction in MS patients, and to characterize patients with cerebellar disability.

Methods In this prospective study, 164 (89 relapsing–remitting and 75 progressive) MS patients and 53 healthy controls were enrolled. Subjects underwent 3T MRI with sequences for assessing lesions and atrophy in cerebellum, supratentorial brain, brainstem and cervical cord. Cerebellar peduncle diffusion-tensor metrics were also derived. Random forest models identified MRI predictors of Expanded Disability Status Scale (EDSS) score and cognition *z*-score. Hierarchical clustering was applied on MRI metrics in patients with cerebellar disability.

Results In MS patients, predictors of higher EDSS score (out-of-bag-$R^2 = 0.83$) were: lower cord grey matter (GM) and global areas, brain volume, GM volume (GMV), cortical GMV, cerebellum lobules I–IV and vermis GMV; and higher cord GM and brainstem lesion volume (LV). Predictors of lower cognition *z*-score (out-of-bag-$R^2 = 0.25$) were: higher supratentorial and superior cerebellar peduncle LV; and lower brain, thalamus and basal ganglia volumes, GMV, cerebellum lobule VIIIb and Crus II GMV. In patients with cerebellar disability, we found three clusters with homogenous MRI metrics: patients with high brain lesion volumes (including cerebellar peduncles), those with marked cerebellum GM atrophy and patients with severe cord damage.

Conclusions Damage to cerebellum GM and connecting structures has a relevant role in explaining cognitive dysfunction and physical disability in MS. Data-driven MRI clustering might improve our knowledge of MRI-clinical correlations.

Keywords Multiple sclerosis · MRI · DWI · Volumetric MRI · Cerebellum

Abbreviations

MS	Multiple sclerosis
RRMS	Relapsing–remitting multiple sclerosis
PMS	Progressive multiple sclerosis
HC	Healthy controls
GM	Grey matter
WM	White matter
FA	Fractional anisotropy
MD	Mean diffusivity
DT	Diffusion tensor
EDSS	Expanded Disability Status Scale
EDSS-C	EDSS cerebellar functional system score
BRB-N	Brief Repeatable Battery of Neuropsychological tests
T2-LV	T2-hyperintense lesion volume
pT2-LV	Percentage T2-hyperintense lesion volume
NBV	Normalized brain volume
GMV	Grey matter volume
CSC	Cervical spinal cord
SD	Standard deviation

✉ Maria A. Rocca
rocca.mara@hsr.it

1 Neuroimaging Research Unit, Division of Neuroscience, IRCCS San Raffaele Scientific Institute, Milan, Italy

2 Neurology Unit, IRCCS San Raffaele Scientific Institute, Milan, Italy

3 Neurorehabilitation Unit, IRCCS San Raffaele Scientific Institute, Milan, Italy

4 Neurophysiology Service, IRCCS San Raffaele Scientific Institute, Milan, Italy

5 Vita-Salute San Raffaele University, Milan, Italy

IQR Interquartile range
OOB Out-of-bag

Introduction

Cerebellar signs are common in multiple sclerosis (MS) patients [27, 44]. In addition to its well-established role in motor coordination, the cerebellum has an increasingly recognized contribution in cognitive performance [27, 44].

In the cerebellum of MS patients, pathological evidence showed extensive white matter (WM) and grey matter (GM) damage, especially in patients with progressive MS (PMS) [19, 21]. MRI studies confirmed higher cortical lesion number and volume in PMS compared to relapsing–remitting (RR) MS patients [7] and more prominent GM atrophy with increasing disability [30]. Regarding correlations with physical disability and cognitive impairment, while earlier studies focused on MRI measures of WM vs GM damage [2, 3], more recent studies investigated lobular patterns of cerebellar GM damage. Consistently with their functional specialization [37], damage to anterior lobes correlated with physical disability and involvement of posterior lobes correlated with cognitive impairment [11, 13, 26]. Functional plasticity mechanisms occurring in the cerebellum may contribute to compensate for MS structural damage [10, 35].

The cerebellum is a highly interconnected structure, whose functioning is critically dependent onto input and output pathways [37, 38]. Cortico-ponto-cerebellar (passing through middle cerebellar peduncle [MCP]) and cerebello-thalamo-cortical (through superior cerebellar peduncle [SCP]) pathways participate to motor control and cognitive functions. Spino-cerebellar (through inferior cerebellar peduncle [ICP]) and cerebello-spinal (through MCP) pathways provide rapid balance, posture and movement control [37]. Diffusion tensor (DT) MRI measures of microstructural damage of MCP and SCP better differentiated patients with and without cerebellar symptoms, compared with cerebellar T2-hyperintense lesion volume (T2-LV) and atrophy [30].

Our study rationale was twofold. First, we applied a multiparametric MRI approach (lesions, atrophy and microstructural abnormality quantification) evaluating cerebellum, brain and cervical spinal cord (CSC), to detect abnormalities of these structures and to identify predictors of physical disability and cognitive impairment in MS patients according to their clinical phenotype. Second, hypothesizing that damage to input and output pathways might partly explain cerebellar symptoms/signs in MS, we applied a data-driven clustering technique on previous MRI variables in patients with cerebellar disability, to identify the main pathophysiological mechanisms underlying clinically evident cerebellar dysfunction.

Materials and methods

Ethics committee approval

The local ethical standards committee on human experimentation approved this hypothesis-driven analysis of prospectively acquired data. Written informed consent was obtained from all participants.

Subjects and clinical assessment

From June 2017 to January 2020, we consecutively enrolled 164 MS patients [39] and 53 healthy controls (HC), as detailed in Fig. 1 and Supplemental methods. On the day of MRI acquisition, all subjects underwent neurological examination with assessment of clinical phenotype [23] and Expanded Disability Status Scale (EDSS) score, and neuropsychological evaluation, with the Brief Repeatable Battery of Neuropsychological tests (BRB-N) [31]. Domain specific and global cognition (BRB-N) *z*-scores were calculated as detailed in Supplemental Methods.

MRI acquisition

Using a 3.0 Tesla Philips scanner, the following sequences of the brain were acquired: 3D T2-weighted fluid-attenuated inversion-recovery, T2-weighted turbo spin echo, T1-weighted turbo field echo, and diffusion-weighted imaging. During the same scanning session, the following CSC sequences were obtained: 3D T1-weighted turbo field echo, T2-weighted fast field echo, and 2D phase-sensitive inversion recovery (PSIR) at the C2-C3 intervertebral disk level. See Supplemental Methods for sequence geometry details.

MRI analysis

T2-LV was calculated using a fully automated approach using 3D FLAIR and 3D T1-weighted sequences [41]. For the whole brain, supratentorial brain, brainstem, cerebellum GM, and cerebellum WM, a "percentage T2-LV" (pT2-LV) was calculated dividing T2-LV by the volume of the same region (see below), indicating the percentage of tissue affected by lesions.

On 3D T1-weighted lesion-filled images [42], normalized brain, GM, cortical GM and WM volumes were calculated using SIENAX software. Automated segmentation of the thalamus and basal ganglia (caudate, putamen, pallidum and accumbens) was performed using FIRST software [28]. Volume of these structures was multiplied by the head-normalization factor derived from SIENAX, and summated between

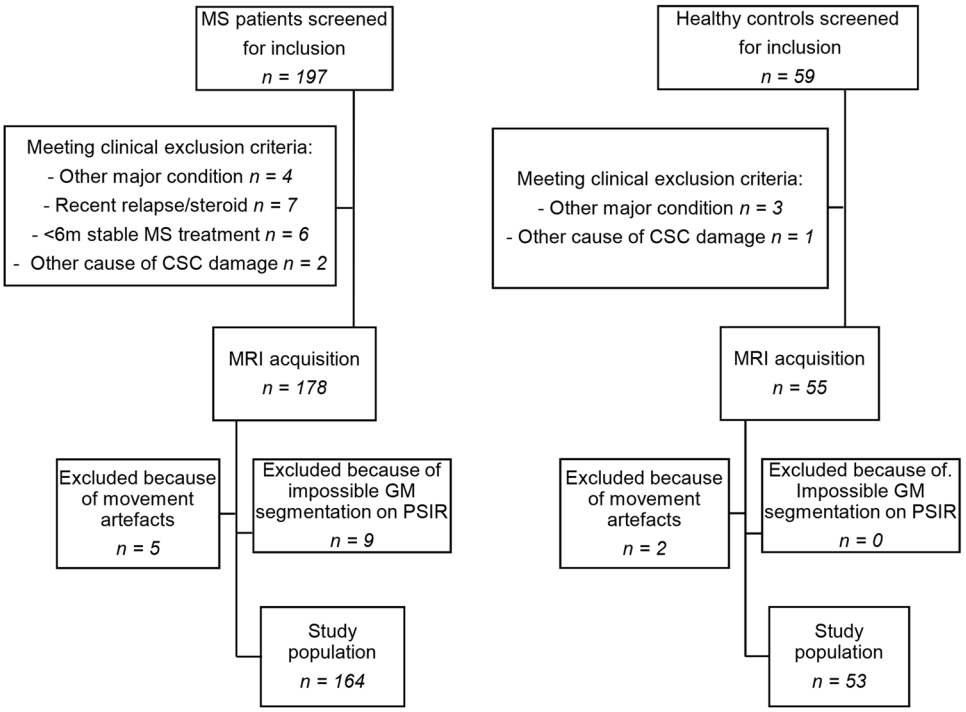

Fig. 1 Study flow-chart. This figure illustrates enrollment of MS patients and healthy controls. *MS* multiple sclerosis, *CSC* cervical spinal cord, *GM* grey matter, *PSIR* phase-sensitive inversion recovery

left and right sides. The thalamus was considered separately due to its role in explaining cognitive and motor deficits in MS [25] and in cerebello-thalamo-cortical connections [37].

Cerebellar volumes were calculated using the Spatially Unbiased Infratentorial Toolbox (SUIT), which is a dedicated tool for the accurate segmentation of posterior fossa structures [16]. Lobular volumes were computed as the sum of their right and left hemispheric portions. Anterior and posterior cerebellar volumes were calculated as the sum of lobules I–V and VI–X, respectively. Cerebellar vermis was considered separately.

Diffusion-weighted MRI analysis

Diffusion-weighted images were pre-processed for correcting movement and distortions, and fractional anisotropy (FA) and mean diffusivity (MD) maps were derived for each subjects. Then, an in-house WM atlas was used for extracting DT metrics in each cerebellar peduncle. Given the symmetry of EDSS cerebellar functional system score (EDSS-C), we averaged DT metrics for left and right tracts before statistical analysis (see Supplemental Methods for more details on analysis).

CSC MRI analysis

CSC MRI analysis was performed as previously described [6], obtaining pT2-LV between C1 and C5 vertebral levels for the whole CSC, the GM, and dorsal columns (which include spinocerebellar pathways); and cross-sectional area (below just "area") of the global CSC and GM at C2–C3 vertebral level. Intra- and inter-rater reliability for manual GM area assessments showed intra-class correlation coefficients of 0.98 and 0.90 [6].

Statistical analysis

Continuous demographic and clinical variables were compared between groups using a two-sample *t*-test or Mann–Whitney test, according to variable distribution. The chi-square test was applied for categorical data.

All T2-LV measures underwent square-root transformation. Cerebellar volumes were head-size corrected by building an age- and sex-adjusted linear model between raw cerebellar volume and inverse of SIENAX head-normalization factor in HC. The estimated regression coefficient was used for adjusting cerebellar volume. The ratio between adjusted and raw cerebellar volume was used for scaling raw volumes of cerebellar lobules, preserving their additive properties. All MRI variables were compared using age- and sex-adjusted linear models, false-discovery rate (Benjamini–Hochberg procedure) corrected [5]. Given the longer disease duration in PMS patients, we retested the PMS vs RRMS contrast, including disease duration as additional covariate in a sensitivity analysis.

Random forest regression models were performed to identify MRI variables associated with physical EDSS score and cognition *z*-score in all MS, RRMS and PMS patients, including age, sex, disease duration and phenotype in the analyses for adjustment purposes. To gain more insight into

MRI predictors of performance in each cognitive domain, we built similar models identifying MRI variables associated with the *z*-score of each cognitive domain in all MS patients. For each model, 10,000 regression trees were built on a random subset of covariates, with a bootstrap resampling of the observations. A permutation test (1000 permutations) of the outcome was applied to assess feature relevance, providing an unbiased measure of variable importance and significance *p* values for each predictor [1]. The goodness of fit of a new model, trained using only the selected predictors ($p < 0.05$), was expressed by the out-of-bag (OOB)-R^2, the coefficient of multiple determination computed on the left-out observations.

To study the substrates of cerebellar disability, we ran a random forest classification model for identifying MRI variables associated with an EDSS-C ≥ 2, adjusting for age, sex, disease duration and phenotype. The model OOB-accuracy was reported. In accordance with a previous study [22], this cut-off was selected to include only patients with end-stage damage (i.e., disability) to the cerebellar system, to prevent MRI analysis from being contaminated by adaptive mechanisms (e.g., plasticity preserving GMV) [34], which may be prominent in patients with cerebellar signs but no disability (i.e., EDSS-C = 1). Furthermore, we applied a data-driven clustering technique on MS patients having EDSS-C ≥ 2. We ran a principal components analysis on all MRI variables, for dimensionality reduction. The first eight components, showing eigenvalues greater than one, according to Kaiser's rule, and capturing 81% of the variance, were retained. These latent variables were finally used to perform an agglomerative hierarchical clustering analysis, using Ward linkage, in MS patients with cerebellar disability. The optimal number of clusters was determined by a consensus voting approach across 23 different indices using NBclust R package [9]. Differences among clusters in demographic, clinical and MRI variables were assessed by false-discovery rate corrected [5] Kruskal–Wallis and pairwise Wilcoxon rank-sum tests.

For all analyses, statistical significance was set at $p < 0.05$ (SAS Software, version 9.4, and R Software, version 4.0.3).

Data availability statement

The anonymized dataset used and analyzed during the current study is available from the corresponding author on reasonable request.

Results

Clinical characteristics

The study included 164 MS (89 RRMS, 75 PMS) patients (97 women aged 21–70 years [mean 44 years] and 67 men aged 20–71 years [mean 45 years]) and 53 HC (26 women aged 19–72 years [mean 43 years] and 27 men aged 19–71 years [mean 44 years]) (Fig. 1). Table 1 summarizes their main demographic and clinical characteristics.

MRI variables

Table 2 summarizes results of MRI analyses and between-group comparisons. Compared to HC, RRMS patients had reduced volume of all examined global brain, supratentorial and infratentorial structures ($p \leq 0.001$), except for brain, cortical and cerebellar GMV. Compared to HC and RRMS, PMS patients had reduced volume of all global brain, supratentorial and infratentorial structures ($p < 0.001$).

In the cerebellum, compared to HC, RRMS patients had reduced GMV of posterior lobe ($p = 0.02$), Crus II ($p = 0.01$), lobule VIIb ($p = 0.02$) and lobule X ($p = 0.05$), whereas PMS patients had reduced GMV of both lobes, vermis and all single lobules ($p < 0.001$). Compared to RRMS, PMS patients showed reduced GMV in all cerebellar compartments (*p* ranging from 0.005 to < 0.001). Compared to HC, RRMS and PMS patients had increased SCP, MCP and ICP MD (*p* ranging from < 0.001 to 0.04). PMS patients also had reduced SCP ($p = 0.04$), MCP ($p = 0.03$) and ICP ($p < 0.001$) FA. Compared to RRMS, PMS patients showed reduced ICP FA ($p = 0.01$) and increased ICP MD ($p = 0.003$).

Compared to HC, both groups of MS patients had reduced global and GM CSC areas (*p* ranging from 0.004 to < 0.001). Compared to RRMS, PMS patients had higher global, dorsal column and GM CSC pT2-LV and reduced global and GM CSC areas ($p < 0.001$).

After adjusting for disease duration, significant differences between PMS and RRMS patients survived in terms of GM atrophy in all explored areas, brainstem global CSC atrophy, infratentorial and CSC pT2-LV, and ICP microstructural damage, while WM atrophy and supratentorial pT2-LV became not significant (Table 2).

Informative predictors of physical disability and cognitive impairment

Table 3 and Fig. 2 summarize results of random forest analysis. In MS patients, predictors of higher EDSS score (OOB-$R^2 = 0.83$) were (in decreasing order of importance): lower CSC GM area, higher CSC GM pT2-LV, lower NBV, lower brain GMV, higher brainstem pT2-LV, lower CSC global area, lower brain cortical GMV, lower cerebellum lobules I–IV and lower vermis GMV. In RRMS patients, predictors of higher EDSS score (OOB-$R^2 = 0.35$) were: higher brainstem and CSC GM pT2-LV, lower CSC global area, higher MCP and cerebellum WM pT2-LV. In PMS patients, predictors of higher EDSS score (OOB-$R^2 = 0.31$) were: lower

Table 1 Main demographic and clinical characteristics of healthy controls and MS patients (as a whole and according to MS clinical phenotype)

	Healthy controls ($n=53$)	MS (n = 164)	MS vs HC p value	RRMS (n = 89)	PMS ($n=75$)	PMS vs RRMS p value
Men/Women	27/26	67/97	0.21$^{\bigcirc}$	37/52	30/45	0.84$^{\bigcirc}$
Age [years]	43 (13)	45 (11)	0.22^{+}	40 (10)	50 (9)	< 0.001^{+}
Median education (IQR) [years]	13 (10–17)	13 (8–17)	0.44*	13 (10–18)	13 (8–16)	0.23*
Median disease duration (IQR) [years]	–	11 (2–21)	–	5 (1–14)	19 (9–24)	< 0.001*
Median EDSS score (IQR)	–	4.5 (1.5–6.0)	–	1.5 (1.0–2.5)	6.0 (5.5–6.5)	< 0.001*
Median EDSS cerebellar functional system score (IQR)	–	0 (0–2)	–	0 (0–0)	2 (1–3)	< 0.001*
Cognition (BRB-N) z-score	–	– 0.69 (0.79)	–	– 0.51 (0.76)	– 0.91 (0.77)	0.001$^{\&}$
Verbal memory z-score	–	– 0.86 (1.10)	–	– 0.73 (1.00)	– 1.03 (1.18)	0.10$^{\&}$
Visuo-spatial memory z-score	–	– 0.18 (0.95)	–	0.06 (0.91)	– 0.47 (0.93)	< 0.001$^{\&}$
Attention z-score	–	– 0.81 (1.08)	–	– 0.60 (0.96)	– 1.07 (1.17)	0.001$^{\&}$
Verbal fluency z-score	–	– 0.85 (1.13)	–	– 0.68 (1.22)	– 1.06 (1.00)	0.04$^{\&}$

Values are reported as mean (standard deviation), unless otherwise specified

MS multiple sclerosis, *RR* relapsing–remitting, *PMS* progressive multiple sclerosis, *EDSS* Expanded Disability Status Scale, *IQR* interquartile range, *BRB-N* Brief Repeatable Battery of Neuropsychological Tests

*Mann–Whitney *U* Test

$^{\&}$linear models

$^{\bigcirc}$Chi-square test

$^{+}$Two-sample *T* test

CSC GM area, lower cerebellum lobules I-IV GMV, lower NBV and lower brain GMV.

In MS patients, predictors of lower cognition z-score (OOB-$R^2 = 0.25$) were: higher supratentorial and SCP pT2-LV, lower NBV, lower thalamus volume, lower cerebellum lobule VIIIb GMV, lower basal ganglia volume, lower brain GMV and lower cerebellum Crus II GMV. In RRMS patients, predictors of lower cognition z-score (OOB-$R^2 = 0.18$) were: lower thalamus volume, higher supratentorial and SCP pT2-LV, lower NBV, lower posterior cerebellum and cerebellum Crus II GMV, and higher cerebellum WM pT2-LV. In PMS patients, predictors of lower cognition z-score (OOB-$R^2 = 0.22$) were: lower basal ganglia volume, lower brain GMV, lower cerebellum lobule VIIIb GMV, lower thalamus volume, higher supratentorial and lower cerebellum Crus II GMV.

MRI predictors of EDSS-C ≥ 2 and cognitive domain-specific z-scores were also investigated in MS patients, as reported in Table 4.

Characteristics of MS patients with cerebellar disability

Supplementary Table 1 summarizes clinical and MRI characteristics of MS patients with cerebellar disability. According to the optimal number of clusters criterion (as suggested by 13 out of 23 indices), 3 groups of MS patients with cerebellar disability were identified from data-driven hierarchical clustering of MRI variables. The first cluster, including 18 patients and the highest percentage of RRMS patients ($n=4$, 22%), was named "lesions" due to highest supratentorial T2-LV and high T2-LV in infratentorial compartments. The second cluster, including 24 patients (2, 8%, RRMS), was named "cerebellum" due to marked cerebellum GMV reduction compared to the others. The third cluster, including 14 PMS and no RRMS patients, was named "cord" due to worst CSC damage, in terms of both highest CSC pT2-LV and lowest CSC GM area.

Figure 3 summarizes differences in demographic and clinical variables between groups. "Cerebellum" patients (mean age = 54, SD = 7 years) were older compared to "lesions" (mean age = 50, SD = 11 years; $p=0.05$) and "cord" (mean age = 46, SD = 10 years; $p=0.02$) patients. Sex, EDSS and EDSS-C had similar distributions among groups. "Cord" patients had shorter disease duration (median = 17, IQR = 10–20 years) compared to "cerebellum" patients (median = 23, IQR = 19–27 years; $p=0.02$) but not to "lesions" patients (median = 20, IQR = 16–25 years; $p=0.21$). "Lesions" and "cerebellum" patients had similar cognitive function compared to each other, while they had worse cognitive function compared to "cord" patients ($p=0.01$ and $p=0.03$, respectively).

Figure 4 summarizes between-group differences in MRI variables. NBV, brain GMV and WMV, thalamus

Table 2 Main MRI metrics in healthy controls and MS patients and between-group comparisons

Variable	Healthy controls ($n=53$)	RRMS ($n=89$)	PMS ($n=75$)	RRMS vs healthy controls		PMS vs healthy controls		PMS vs RRMS	
	Mean (SD)	Mean (SD)	Mean (SD)	Estimated mean difference (95% CI)	p_{FDR}	Estimated mean difference (95% CI)	p_{FDR}	Estimated mean difference (95% CI)	p_{FDR}
Global brain measures [mL]									
T2-LV	0.00[#] (0.00–0.26)	2.11[#] (0.88–5.37)	4.88[#] (1.78–12.26)	1.45[+] (1.22, 1.67)	< 0.001	2.18[+] (1.81, 2.54)	< 0.001	0.73[+] (0.32, 1.14)	0.001*
NBV	1564 (41)	1535 (64)	1472 (58)	– 26 (– 40, – 11)	0.001	– 67 (– 84, – 49)	< 0.001	– 41 (– 59, – 22)	< 0.001*
GMV	872 (39)	864 (42)	818 (41)	– 6 (– 16, 5)	0.29	– 30 (– 43, – 17)	< 0.001	– 25 (– 37, – 12)	< 0.001*
WMV	691 (29)	670 (34)	654 (36)	– 20 (– 30, – 9)	< 0.001	– 34 (– 46, – 21)	< 0.001	– 23 (– 35, – 11)	< 0.001
Supratentorial brain measures									
pT2-LV	0.00[#] (0.00–0.02)	0.19[#] (0.08–0.46)	0.45[#] (0.17–1.03)	0.44[+] (0.37, 0.52)	< 0.001	0.70[+] (0.58, 0.82)	< 0.001	0.25[+] (0.12, 0.39)	0.001
Cortical GMV [mL]	655 (33)	649 (37)	615 (33)	– 4 (– 13, 6)	0.44	– 22 (– 33, – 11)	< 0.001	– 18 (– 28, – 8)	0.001*
Thalamus Volume [mL]	22.5 (1.2)	20.9 (2.2)	18.9 (2.3)	– 1.5 (– 2.0, – 1.0)	< 0.001	– 3.0 (– 3.7, – 2.4)	< 0.001	– 1.5 (– 2.3, – 0.8)	< 0.001*
Basal Ganglia Volume [mL]	29.1 (1.9)	27.6 (2.8)	25.5 (3.2)	– 1.5 (– 2.3, – 0.8)	< 0.001	– 3.0 (– 4.0, – 2.1)	< 0.001	– 1.5 (– 2.8, – 0.8)	< 0.001*
Infratentorial brain measures									
Brainstem pT2-LV	0.00[#] (0.00–0.00)	0.30[#] (0.00–0.62)	0.70[#] (0.31–1.56)	–	–	–	–	0.43[+] (0.20, 0.66)	0.001*
Brainstem Volume [mL]	30.8 (2.6)	29.2 (2.3)	27.1 (2.7)	– 1.5 (– 2.4, – 0.7)	< 0.001	– 3.3 (– 4.4, – 2.4)	< 0.001	– 1.8 (– 2.7, – 1.0)	< 0.001*
Cerebellum GM pT2-LV	0.00[#] (0.00–0.00)	0.01[#] (0.00–0.06)	0.02[#] (0.00–0.10)	–	–	–	–	0.06[+] (0.01, 0.12)	0.05
Cerebellum GMV [mL]	104.7 (10.0)	102.0 (8.9)	92.2 (9.6)	– 2.1 (– 5.2, 1.0)	0.20	– 8.2 (– 11.8, – 4.6)	< 0.001	– 6.1 (– 9.0, – 3.3)	< 0.001*
Cerebellum WM pT2-LV	0.00[#] (0.00–0.00)	0.17[#] (0.00–0.44)	0.32[#] (0.08–0.99)	–	–	–	–	0.31[+] (0.12, 0.50)	0.003*
Cerebellum WMV [mL]	23.8 (2.1)	22.6 (1.9)	22.1 (2.1)	– 1.1 (– 1.7, – 0.4)	0.002	– 1.8 (– 2.5, – 1.0)	< 0.001	– 0.7 (– 1.3, – 0.1)	0.04
Cerebellum GMV [mL]									
Anterior lobe	13.0 (1.3)	12.7 (1.2)	11.4 (1.3)	– 0.2 (– 0.6, 0.1)	0.20	– 0.9 (– 1.3, – 0.5)	< 0.001	– 0.7 (– 1.0, – 0.3)	0.002*
Posterior lobe	90.7 (7.5)	87.3 (7.9)	78.7 (8.4)	– 2.8 (– 5.0, – 0.5)	0.02	– 8.0 (– 10.8, – 5.2)	< 0.001	– 5.2 (– 7.7, – 2.8)	< 0.001*
Lobules I–IV	5.6 (0.6)	5.4 (0.6)	4.8 (0.6)	– 0.1 (– 0.3, 0.0)	0.14	– 0.4 (– 0.7, – 0.2)	< 0.001	– 0.3 (– 0.5, – 0.1)	0.001*
Lobule V	7.4 (0.7)	7.2 (0.6)	6.6 (0.7)	– 0.1 (– 0.3, 0.1)	0.29	– 0.4 (– 0.7, – 0.2)	< 0.001	– 0.3 (– 0.5, – 0.1)	0.004*
Lobule VI	16.2 (1.5)	15.7 (1.4)	14.3 (1.6)	– 0.3 (– 0.8, 0.1)	0.14	– 1.2 (– 1.8, – 0.7)	< 0.001	– 0.9 (– 1.4, – 0.4)	0.001*
Lobule VIIa Crus I	22.6 (2.2)	21.9 (2.2)	19.6 (2.2)	– 0.6 (– 1.2, 0.0)	0.08	– 1.9 (– 2.7, – 1.1)	< 0.001	– 1.3 (– 2.0, – 0.6)	0.001*

Table 2 (continued)

Variable	Healthy controls ($n=53$)	RRMS ($n=89$)	PMS ($n=75$)	RRMS vs healthy controls		PMS vs healthy controls		PMS vs RRMS	
	Mean (SD)	Mean (SD)	Mean (SD)	Estimated mean difference (95% CI)	p_{FDR}	Estimated mean difference (95% CI)	p_{FDR}	Estimated mean difference (95% CI)	p_{FDR}
Lobule VIIa Crus II	16.4 (1.5)	15.6 (1.7)	14.3 (1.7)	– 0.7 (– 1.2, – 0.2)	0.01	– 1.5 (– 2.1, – 0.9)	< 0.001	– 0.8 (– 1.3, – 0.3)	0.005*
Lobule VIIb	9.0 (0.8)	8.6 (0.9)	7.8 (0.9)	– 0.3 (– 0.6, – 0.1)	0.02	– 0.8 (– 1.2, – 0.5)	< 0.001	– 0.5 (– 0.8, – 0.2)	0.001*
Lobule VIIIa	8.7 (0.7)	8.4 (0.8)	7.6 (0.9)	– 0.3 (– 0.5, 0.0)	0.06	– 0.8 (– 1.1, – 0.4)	< 0.001	– 0.5 (– 0.8, – 0.3)	< 0.001*
Lobule VIIIb	6.7 (0.6)	6.4 (0.7)	5.7 (0.8)	– 0.2 (– 0.4, 0.0)	0.10	– 0.6 (– 0.9, – 0.4)	< 0.001	– 0.4 (– 0.7, – 0.2)	< 0.001*
Lobule IX	5.5 (0.7)	5.3 (0.9)	4.6 (0.8)	– 0.2 (– 0.5, 0.0)	0.09	– 0.7 (– 1.0, – 0.4)	< 0.001	– 0.5 (– 0.7, – 0.2)	0.001*
Lobule X	0.92 (0.14)	0.87 (0.13)	0.73 (0.17)	– 0.04 (– 0.08, 0.00)	0.05	– 0.13 (– 0.18, – 0.07)	< 0.001	– 0.08 (– 0.13, – 0.04)	0.001*
Vermis	4.7 (0.4)	4.5 (0.5)	4.1 (0.4)	– 0.1 (– 0.2, 0.0)	0.17	– 0.4 (– 0.5, – 0.2)	< 0.001	– 0.3 (– 0.4, – 0.1)	< 0.001*
Cerebellar peduncle pT2-LV									
SCP	0.00# (0.00–0.00)	8.82# (2.55–23.00)	25.61# (5.34–80.31)	–	–	–	–	1.64+ (0.56–2.72)	0.005*
MCP	0.00# (0.00–0.00)	1.80# (0.00–3.89)	4.24# (1.30–9.41)	–	–	–	–	1.06+ (0.51–1.60)	< 0.001*
ICP	0.00# (0.00–0.00)	0.56# (0.00–6.23)	3.48# (0.00–10.68)	–	–	–	–	0.98+ (0.31–1.65)	0.006*
Cerebellar peduncle FA									
SCP	0.63 (0.04)	0.62 (0.04)	0.61 (0.04)	– 0.01 (– 0.02, 0.01)	0.36	– 0.02 (– 0.03, – 0.01)	0.04	– 0.01 (– 0.02, 0.01)	0.28
MCP	0.55 (0.03)	0.54 (0.03)	0.53 (0.04)	– 0.01 (– 0.02, 0.00)	0.09	– 0.01 (– 0.03, – 0.01)	0.03	– 0.01 (– 0.02, 0.01)	0.36
ICP	0.52 (0.06)	0.50 (0.06)	0.46 (0.06)	– 0.02 (– 0.04, 0.00)	0.12	– 0.04 (– 0.06, – 0.02)	< 0.001	– 0.03 (– 0.05, – 0.01)	0.01*
Cerebellar peduncle MD [$mm^2/s \times 10^{-3}$]									
SCP	0.93 (0.06)	0.96 (0.07)	0.98 (0.10)	0.03 (0.00, 0.05)	0.03	0.05 (0.02, 0.08)	0.02	0.03 (0.00, 0.05)	0.09
MCP	0.80 (0.04)	0.83 (0.04)	0.85 (0.06)	0.02 (0.01, 0.04)	0.04	0.04 (0.02, 0.06)	< 0.001	0.02 (0.00, 0.03)	0.08
ICP	0.98 (0.12)	1.04 (0.13)	1.12 (0.14)	0.05 (0.01, 0.09)	0.03	0.13 (0.07, 0.18)	< 0.001	0.08 (0.03, 0.13)	0.003*
CSC pT2-LV									
Global	0.00# (0.00–0.00)	1.78# (0.58–3.60)	5.28# (3.53–7.82)	–	–	–	–	1.04+ (0.77–1.31)	< 0.001*
GM	0.00# (0.00–0.00)	1.01# (0.00–2.38)	3.65# (1.86–8.01)	–	–	–	–	1.11+ (0.77–1.45)	< 0.001*
Dorsal columns	0.00# (0.00–0.00)	1.27# (0.00–5.84)	6.00# (2.11–9.61)	–	–	–	–	1.16+ (0.74–1.59)	< 0.001*

Table 2 (continued)

Variable	Healthy controls ($n=53$)	RRMS ($n=89$)	PMS ($n=75$)	RRMS vs healthy controls		PMS vs healthy controls		PMS vs RRMS	
	Mean (SD)	Mean (SD)	Mean (SD)	Estimated mean difference (95% CI)	p_{FDR}	Estimated mean difference (95% CI)	p_{FDR}	Estimated mean difference (95% CI)	p_{FDR}
CSC area [mm^2]									
Global	87.7 (8.6)	80.4 (9.6)	71.0 (9.9)	– 6.8 (– 9.7, – 3.9)	< 0.001	– 15.7 (– 19.2, – 12.2)	< 0.001	– 8.9 (– 12.1, – 5.7)	< 0.001*
GM	13.0 (1.0)	12.4 (1.0)	9.6 (1.2)	– 0.6 (– 1.0, – 0.2)	0.004	– 3.2 (– 3.7, – 2.7)	< 0.001	– 2.6 (– 3.0, – 2.2)	< 0.001*

Values are reported as mean (standard deviation), unless otherwise specified

RRMS relapsing–remitting multiple sclerosis, *PMS* progressive multiple sclerosis, p_{FDR} false-discovery rate (FDR)-corrected *p* value, *CI* confidence interval, *NBV* normalized brain volume, *GMV* grey matter volume, *WMV* white matter volume, *T2-LV* T2-hyperintense lesion volume, *pT2-LV* percentage T2-hyperintense lesion volume, *GM* grey matter, *WM* white matter, *ICP* inferior cerebellar peduncle, *MCP* middle cerebellar peduncle, *SCP* superior cerebellar peduncle, *FA* fractional anisotropy, *MD* mean diffusivity, *CSC* cervical spinal cord

*False-discovery-rate (FDR)-corrected $p<0.05$ at sensitivity analysis (linear models adjusted for disease duration, in addition to age and sex)

#Median (interquartile range)

+On square-root scale

Statistical methods: age- and sex-adjusted linear models; false-discovery rate (FDR) correction was applied to adjust for the overall number of pairwise contrasts (Benjamini–Hochberg procedure); as sensitivity analysis, the contrast PMS vs RRMS was retested by linear models adjusted for disease duration, in addition to age and sex (significant results are reported in the form of * after the original p value)

volume and brain cortical GMV were similar in "lesions" and "cerebellum" patients, but reduced in "cord" patients ($p \leq 0.01$). Supratentorial pT2-LV was higher in "lesions" compared to "cerebellum" patients ($p=0.01$), and in the latter compared to "cord" patients ($p=0.01$).

Brainstem volume was lowest in "cerebellum" compared to "lesions" ($p=0.01$) and "cord" ($p<0.001$) patients. Likewise, cerebellum GMV volume was lowest in "cerebellum" compared to "lesions" and "cord" ($p<0.001$ for both) patients. Cerebellum lobe and lobule GMV showed similar distributions among groups (data not shown). No differences were observed for cerebellum WMV. Brainstem and cerebellum WM pT2-LV were higher in "lesions" and "cerebellum" compared to "cord" patients ($p<0.05$). Cerebellum GM pT2-LV was higher in "lesions" compared to "cerebellum" ($p=0.03$) and "cord" ($p=0.005$) patients. SCP pT2-LV was higher in "lesions" compared to "cerebellum" patients ($p=0.01$), and in the latter compared to "cord" patients ($p=0.01$). MCP and ICP pT2-LV were higher in "lesions" and "cerebellum" compared to "cord" patients ($p<0.05$). Likewise, cerebellar peduncle MD were higher, and ICP FA was reduced, in "lesions" and "cerebellum" compared to "cord" patients ($p \leq 0.01$).

CSC pT2-LV was higher in "cord" compared to "lesions" ($p=0.02$) and "cerebellum" ($p=0.01$) patients. CSC GM area was reduced in "cord" compared to "lesions" ($p=0.02$) and "cerebellum" ($p=0.01$) patients.

Discussion

This multiparametric MRI study aimed to evaluate in-vivo damage to the cerebellum and its role in explaining physical disability and cognitive impairment in MS. Differently from previous work [2, 3, 7, 11, 13, 26, 30], RRMS and PMS patients were assessed separately, given their known immunological, pathological and MRI differences [12, 19, 21]. Furthermore, we included an assessment of CSC damage, given the central role of spinocerebellar pathways for motor cerebellar functions [37].

Results of between-group comparisons of global brain T2-LV and atrophy measures were in line with existing literature [6, 33]. They confirmed more severe damage in PMS compared to RRMS patients [19, 33]. Cerebellum WMV—but not GMV—was reduced in RRMS patients compared to HC, likely reflecting earlier WM atrophy and an orderly process of GM atrophy in MS [17, 33]. Posterior cerebellum and lobules Crus II, VIIb, X were atrophied in RRMS compared to HC. Crus II and lobule VIIb belong to areas of the cerebellum with known cognitive functions, possibly reflecting the often subclinical nature of cognitive dysfunction in RRMS patients [8, 14]. Lobule X corresponds to the flocculonodular lobe, sitting in close proximity with the forth ventricle, making it susceptible to cerebrospinal fluid-mediated damage [15]. In line with global analysis, all cerebellar compartments were atrophic and showed higher pT2-LV in PPMS compared to RRMS patients. Cerebellar peduncles had abnormal DT-MRI indices in PMS patients

Table 3 Informative predictors of physical disability and cognitive impairment in MS patients

Outcome	MS patients			RRMS patients			PMS patients		
	Statistics	Independent predictors	Relative importance	Statistics	Independent predictors	Relative importance	Statistics	Independent predictors	Relative importance
EDSS score	OOB-$R^2=0.83$	CSC GM area	100	OOB-$R^2=0.35$	Brainstem pT2-LV	100	OOB-$R^2=0.31$	CSC GM area	100
		CSC GM pT2-LV	25.2		CSC GM pT2-LV	99.3		Cerebellum lobules I-IV GMV	60.3
		NBV	16.7		CSC area	63.3		Brain GMV	43.5
		Brain GMV	13.9		MCP pT2-LV	39.2		NBV	35.4
		Brainstem pT2-LV	12.2		Cerebellum WM pT2-LV	31.2			
		CSC area	11.8						
		Brain cortical GMV	11.2						
		Cerebellum lobules I-IV GMV	10.3						
		Cerebellum vermis GMV	8.1						
Cognition (BRB-N) *z*-score	OOB-$R^2=0.25$	Supratentorial pT2-LV	100	OOB-$R^2=0.18$	Thalamus volume	100	OOB-$R^2=0.22$	Basal ganglia volume	100
		SCP pT2-LV	78.2		Supratentorial pT2-LV	97.5		Brain GMV	75.7
		NBV	71.3		SCP pT2-LV	83.8		Cerebellum lobule VIIIb	39.6
		Thalamus volume	48.1		NBV	83.7		Thalamus volume	37.8
		Cerebellum lobule VIIIb GMV	47.4		Posterior cerebellum GMV	68.6		Supratentorial pT2-LV	31.4
		Basal ganglia volume	45.6		Cerebellum lobule VIIa Crus II GMV	58.5		Cerebellum lobule VIIa Crus II GMV	30.4
		Brain GMV	40.9		Cerebellum WM pT2-LV	28.1			
		Cerebellum lobule VIIa Crus II GMV	38.0						

RRMS relapsing–remitting multiple sclerosis, *PMS* progressive multiple sclerosis, *EDSS* Expanded Disability Status Scale, *BRB-N* Brief Repeatable Battery of Neuropsychological Tests, *OOB* out-of-bag, *NBV* normalized brain volume, *GMV* grey matter volume, *pT2-LV* percentage T2-hyperintense lesion volume, *GM* grey matter, *WM* white matter, *MCP* middle cerebellar peduncle, *SCP* superior cerebellar peduncle, *CSC* cervical spinal cord

Statistical methods: random forest analysis adjusted for age, sex, disease duration and phenotype

vs HC, and increased MD in RRMS patients, indicating demyelination and axonal damage [19, 30]. Compared to RRMS, PMS patients showed more severe DT-MRI abnormalities in the ICP, possibly as a consequence of the myelopathy that characterizes PMS, affecting spinocerebellar pathways (the main component of the ICP).

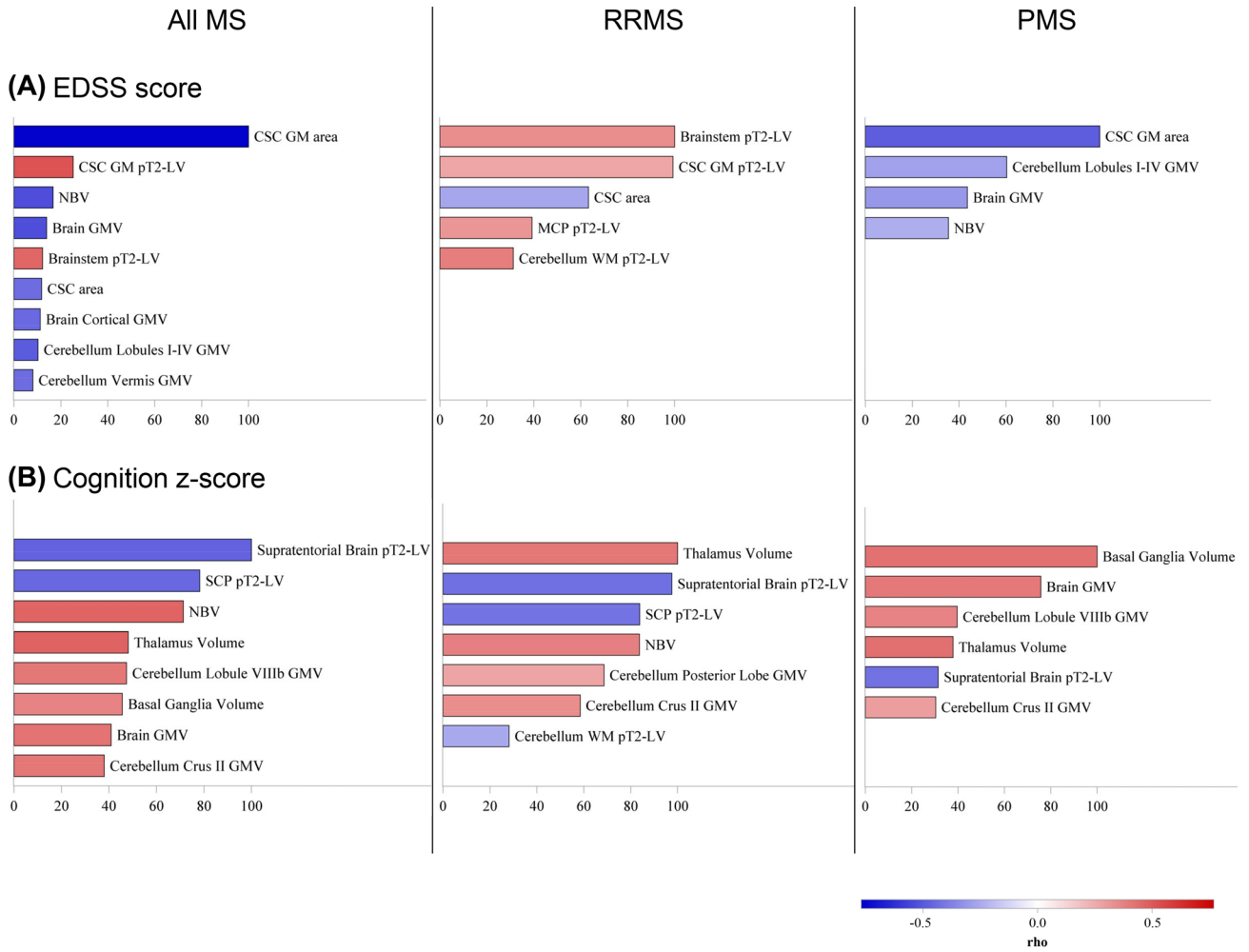

Fig. 2 Informative MRI predictors of physical disability and cognitive function. This figure illustrates informative MRI predictors (random forest analysis, $p < 0.05$) of: **A** EDSS score; **B** cognition *z*-score. Analysis was performed for all MS patients (left column), RRMS patients (middle column) and PMS patients (right column). Relative importance of MRI predictors is represented by the width on the *x*-axis of the bar corresponding to the predictor. Color of bars reflects the strength of association of the predictor with the dependent variable, as quantified by Spearman ρ (white to red for positive associations, white to blue for negative associations). *MS* multiple sclerosis, *RRMS* relapsing–remitting multiple sclerosis, *PMS* progressive multiple sclerosis, *NBV* normalized brain volume, *GMV* grey matter volume, *pT2-LV* percentage T2-hyperintense lesion volume, *GM* grey matter, *WM* white matter, *MCP* middle cerebellar peduncle, *SCP* superior cerebellar peduncle, *CSC* cervical spinal cord

Interestingly, even after adjusting for disease duration, MRI variables investigating damage to brain GM, infratentorial and CSC compartments were significantly more affected in PMS vs RRMS patients, pointing towards a disproportional relevance of damage to these areas in determining the PMS phenotype.

Random forest analysis underscored the central role of CSC GM pT2-LV and atrophy in explaining physical disability in MS patients, in agreement with existing literature [6, 36]. Brain GMV and NBV reduction were also relevant, though their relative importance was lower compared to CSC metrics [33]. Finally, higher brainstem pT2-LV and reduced cerebellar GMV (especially cerebellum lobules I-IV and vermis) predicted worse physical disability, in line with a body of evidence implicating the anterior cerebellar lobe and the vermis—and their connections through the brainstem—in motor function [11, 13, 30, 37, 44]. Furthermore, CSC GM atrophy, SCP pT2-LV, cerebellum GMV, cerebellum lobule VIIa Crus II GMV and brainstem volume and pT2-LV emerged as informative predictors of cerebellar disability, pointing towards damage to infratentorial and CSC areas as determinant for cerebellar-type physical disability (see below for further discussion).

Random forest analysis also confirmed the centrality of supratentorial brain damage in explaining worse global

Table 4 Informative predictors of cerebellar disability (EDSS-C ≥ 2) and performance in each cognitive domain in MS patients

Outcome	MS patients		
	Statistics	Independent predictors	Relative importance
EDSS-C ≥ 2	OOB-Accuracy = 0.87	CSC GM area	100
		SCP pT2-LV	56.7
		Cerebellum GMV	48.9
		Cerebellum lobule VIIa Crus II GMV	23.8
		Brainstem volume	20.9
		Brainstem pT2-LV	20.4
Verbal memory z-score	OOB-R^2 = 0.14	Thalamus volume	100
		Supratentorial pT2-LV	76.3
		Cerebellum lobule VIIIb GMV	58.3
		Brain GMV	51.5
		Brain cortical GMV	49.9
Visuo-spatial memory z-score	OOB-R^2 = 0.24	SCP pT2-LV	100
		Cerebellum posterior lobe GMV	95.1
		Supratentorial pT2-LV	91.3
		Cerebellum lobule VIIa Crus II GMV	80.5
		Cerebellum lobule VIIIb GMV	72.8
		NBV	68.6
Attention z-score	OOB-R^2 = 0.24	Brain GMV	100
		Brain cortical GMV	48.1
		SCP pT2-LV	46.2
		Supratentorial pT2-LV	44.1
		Cerebellum lobule VIIa Crus II GMV	39.8
		Cerebellum lobule VIIIb GMV	32.3
Verbal fluency z-score	OOB-R^2 = 0.17	SCP pT2-LV	100
		Thalamus volume	81.9
		Supratentorial pT2-LV	71.6
		MCP pT2-LV	74.8
		NBV	72.3

MS multiple sclerosis, *OOB* out-of-bag, *EDSS-C* Expanded Disability Status Scale cerebellar functional system score, *CSC* cervical spinal cord, *GM* grey matter, *NBV* normalized brain volume, *GMV* grey matter volume, pT2-*LV* percentage T2-hyperintense lesion volume, *MCP* middle cerebellar peduncle, *SCP* superior cerebellar peduncle

Statistical methods: random forest analysis adjusted for age, sex, disease duration and phenotype

cognitive function in MS patients. Supratentorial T2-LV was the most important predictor, reflecting the fundamental role of WM lesions for cognitive dysfunction in MS, possibly causing a disconnection syndrome [24, 32]. SCP pT2-LV emerged as the second most relevant predictor, supporting: (1) a relevant role of cerebellar damage in cognitive impairment in MS; (2) the central role of damage to philologically important, non-redundant, long WM pathways in determining clinical deficits in MS patients [24]. Other relevant predictors of cognitive functioning were atrophy of the whole brain and deep GM [4, 14], and posterior cerebellum GM [11, 13, 26]. Cerebellum lobule VIIa Crus II was the most consistently implicated lobule, in line with previous evidence on information processing speed in MS

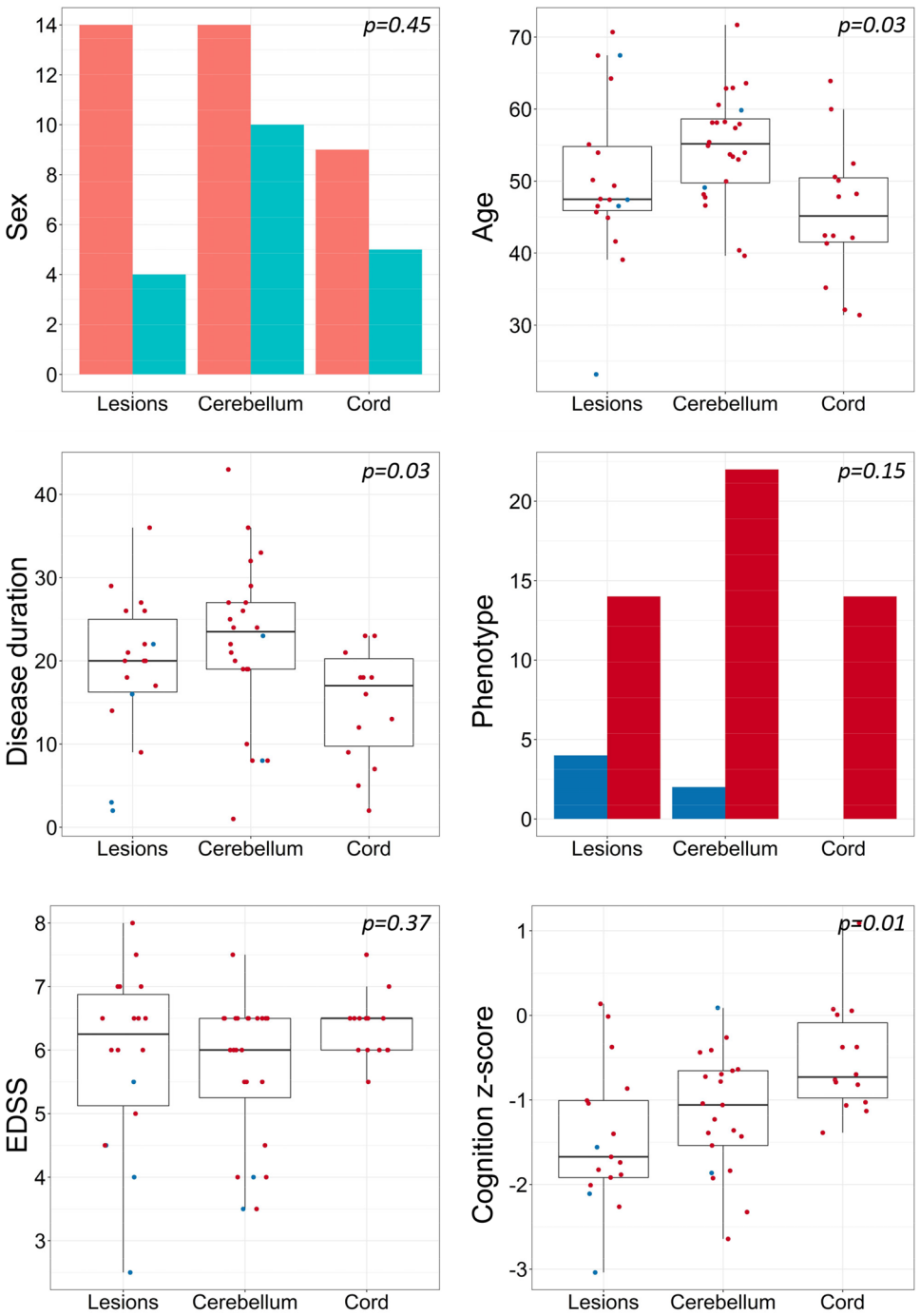

Fig. 3 Group comparisons of demographic and clinical variables among data-driven clusters of MS patients with cerebellar disability. This figure illustrates the distribution of demographic and clinical variables among the 3 clusters of MS patients with cerebellar disability ("lesions", "cerebellum" and "cord" patients). Regarding sex distribution, females are represented in salmon pink and males in green–blue. For the other graphs, RRMS patients are represented as blue dots or bars, and PMS patients as red dots or bars. *EDSS* Expanded Disability Status Scale

patients [26], and cognitive processing in HC [43]. Lobule VIIIb, previously implicated in attention and working memory [37], also emerged as a critical area. In domain-specific random forest analysis, SCP pT2-LV was mainly involved in visuospatial memory, attention and verbal fluency performance; cerebellum lobule VIIa Crus II in visuospatial memory and attention performance; and cerebellum lobule VIIIb in visuospatial memory and attention performance. MCP pT2-LV emerged as an additional predictor of verbal fluency performance in MS patients.

Interestingly, random forest OOB-R^2 index, which reflects the proportion of the variance in the dependent (clinical) variable predictable from independent (MRI) variables, was higher for EDSS than cognition model. This result likely reflects the efficiency of structural MRI techniques assessing lesions, atrophy and WM microstructural damage in grasping MS-related damage to subcortical structures,

which largely impacts on physical disability [19, 33]. Other mechanisms not investigated in this study, such as the presence and efficiency of functional plasticity, might contribute to explain cognitive function [32, 35].

The results of random forest analysis in RRMS and PMS patients showed that different mechanisms contribute to explain disease clinical manifestations in the different stages of the disease. Indeed, lesions played a major role in RRMS, whereas GM atrophy measures were more important in PMS, suggesting a transition from (mainly) a "disconnection syndrome" in RRMS to a neurodegenerative condition in PMS [19, 33].

The second part of the study aimed to shed light on the pathophysiology of cerebellar disability, through data-driven clustering, which is a promising novel tool for understanding MS pathophysiology [18, 40]. Three clusters of MS patients with cerebellar disability were identified: "lesions", "cerebellum", and "cord". "Cord" patients had better cognitive function compared to the other two groups, which is somehow expected, given their less pronounced abnormalities of brain MRI measures. Despite no clinical differences in EDSS score, these clusters of MS patients showed some important differences in MRI metrics. In spite of lower supratentorial pT2-LV, "cerebellum" patients had similar NBV, brain GMV and thalamus volumes compared to "lesions" patients, likely indicating a predisposition to neurodegeneration, at least in part explained by the older age. Likewise, "cerebellum" patients showed lower cerebellum GMV and brainstem volume despite similar infratentorial pT2-LV compared to "lesions" patients, confirming the predisposition to neurodegeneration. Interestingly, "lesions" patients had the highest cerebellum GM pT2-LV, suggesting GM lesions and GM neurodegeneration are two distinct phenomena [20]. DT-MRI metrics of cerebellar peduncles showed similar distributions to brainstem and cerebellum WM pT2-LV, likely reflecting lesion-mediated damage to the normal-appearing WM. Damage to cerebellar peduncles (in terms of focal lesions and microstructural damage) and impaired cerebellum-cortex connectivity (due to supratentorial brain damage) are likely to represent the two pathophysiological mechanisms underlying cerebellar disability in the cluster of "lesions" patients. Instead, it is tempting to hypothesize the cluster of "cerebellum" patients may show a predisposition to neurodenegeration, leading to marked cerebellar atrophy, probably initiated by a significant infratentorial T2-LV, but possibly also mediated by cerebrospinal fluid -vehiculated toxic mediators [15, 19]. Indeed, the cerebellum is a plicated structure, with a high surface area in direct contact with the cerebrospinal fluid. Interestingly, a previous study [29] highlighted the key role of early cerebellar atrophy in predicting a poor prognosis in MS, and an association of cerebellar atrophy with cerebrospinal fluid beta-amyloid burden. On the other hand, "cord" patients had rather isolated CSC damage, with preserved brain, brainstem, and cerebellar volumes, and lower damage to cerebellar peduncles, compared to the other two clusters. This supports a relevant role of spinocerebellar and (indirect) cerebello-spinal pathways in determining cerebellar disability in a subset of MS patients.

This study has clinical relevance. First, damage to the cerebellum, cerebellar peduncles and brainstem predicted physical disability and worse cognition, underscoring the prognostic relevance of infratentorial lesion burden (easily assessable through conventional clinical MRI) for motor and cognitive outcomes. Second, this study delineates the highly heterogenous nature of MS, with complex interplays of different types of damage to several structures in explaining physical disability and cognitive dysfunction. Finally, it clearly separated a subset of MS patients with cerebellar disability and MRI evidence of GM neurodegeneration (namely, "cerebellum" patients), only partly explained by an older age, in agreement with a previous interesting study on beta-amyloid cerebrospinal fluid burden in MS [29]. These patients might benefit from the application of atrophy measures from a proper monitoring of their clinical manifestations.

The study is not without limitations. First, it was cross-sectional, and longitudinal associations between MRI variables and progression of physical disability and cognitive dysfunction remain to be determined. Second, despite pathophysiological similarities, there are also differences between PPMS and SPMS patients, but the small number of PPMS patients did not allow a separate analysis. Third, CSC analysis is still limited by technical issues, limitation to the upper CSC and difficulty in accurately delineating the GM border.

In conclusion, damage to cerebellum GM and connecting structures explains a significant proportion of physical disability and cognitive dysfunction in MS patients, underscoring clinical relevance of posterior fossa lesions and atrophy. Data-driven identification of three MRI-subtypes of patients with cerebellar disability (high brain lesion volumes, cerebellum grey matter atrophy and severe cord damage) might improve our knowledge of MRI-clinical correlations.

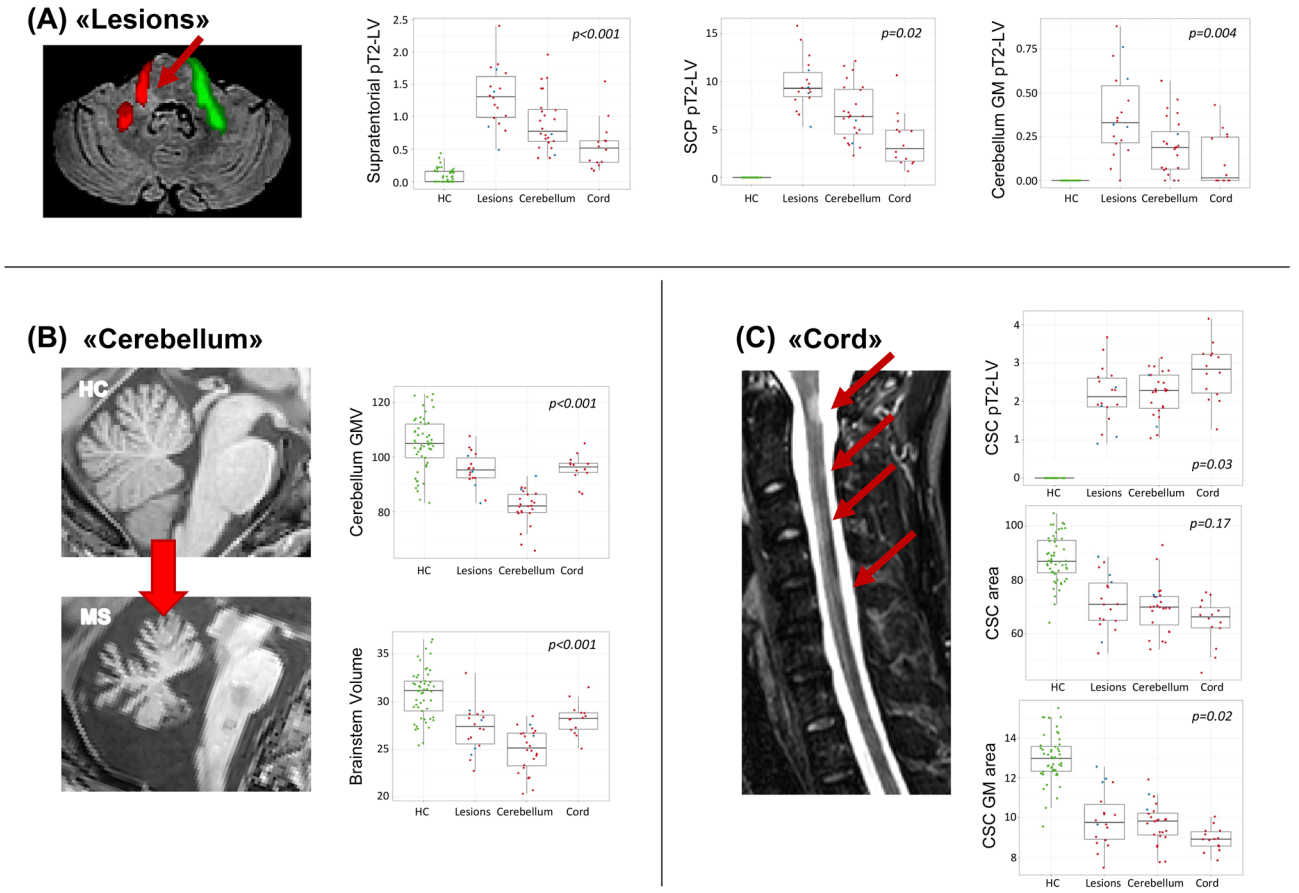
(A) «Lesions»
Supratentorial pT2-LV
p<0.001
SCP pT2-LV
p=0.02
Cerebellum GM pT2-LV
p=0.004
(B) «Cerebellum»
HC
MS
Cerebellum GMV
p<0.001
Brainstem Volume
p<0.001
(C) «Cord»
CSC pT2-LV
p=0.03
CSC area
p=0.17
CSC GM area
p=0.02
HC Lesions Cerebellum Cord

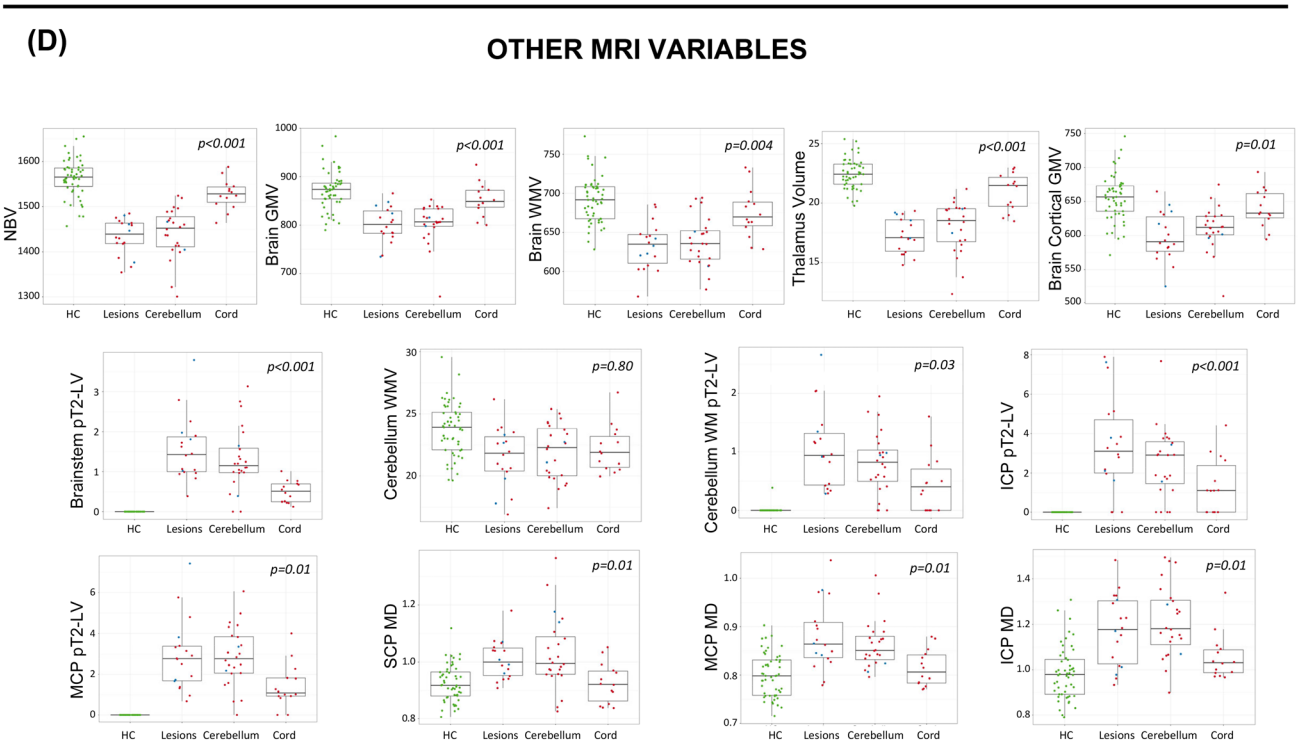
(D)
OTHER MRI VARIABLES
NBV p<0.001
Brain GMV p<0.001
Brain WMV p=0.004
Thalamus Volume p<0.001
Brain Cortical GMV p=0.01
Brainstem pT2-LV p<0.001
Cerebellum WMV p=0.80
Cerebellum WM pT2-LV p=0.03
ICP pT2-LV p<0.001
MCP pT2-LV p=0.01
SCP MD p=0.01
MCP MD p=0.01
ICP MD p=0.01
HC Lesions Cerebellum Cord

◂**Fig. 4** Group comparisons of MRI variables among data-driven clusters of MS patients with cerebellar disability. This figure illustrates the distribution of MRI variables among the 3 clusters of MS patients with cerebellar disability ("lesions", "cerebellum" and "cord" patients). For illustrative purposes, MRI variables were grouped into an upper part, with the 3 clusters and MRI variables most significantly affected in each cluster (**A**–**C**), and a lower part with other MRI variables (**D**). **A** MRI variables most significantly affected in "lesions" patients; **B** MRI variables most significantly affected in "cerebellum" patients; C) MRI variables most significantly affected in "cord" patients; **D** other global brain, supratentorial and infratentorial MRI variables. HC are only shown as a reference group for illustrative purposes. *p* values are derived from Kruskal–Wallis test among groups of MS patients, false discovery rate (FDR) corrected for multiple comparisons. Pairwise comparisons between the groups of patients are reported in the results section. HC are colored in green, RRMS patients in blue, PMS patients in red. All pT2-LV measures are displayed on square-root scale. Each cluster of MS patients is accompanied by an illustrative vignette underscoring the main damage mechanism. Small red arrows highlight MS lesions. *HC* healthy controls, *NBV* normalized brain volume, *GMV* grey matter volume, *WMV* white matter volume, *pT2-LV* ercentage T2-hyperintense lesion volume, *GM* grey matter, *WM* white matter, *ICP* inferior cerebellar peduncle, *MCP* middle cerebellar peduncle, *SCP* superior cerebellar peduncle, *FA* fractional anisotropy, *MD* mean diffusivity, *CSC* cervical spinal cord

Supplementary Information The online version contains supplementary material available at https://doi.org/10.1007/s00415-022-11021-1.

Author contributions RB contributed to study concept, patient recruitment, MRI data analysis, drafting/revising the manuscript. AM contributed to statistical data analysis and drafting/revising the manuscript. EP contributed to the acquisition and analysis of MRI data and revising the manuscript. OM contributed to analysis of neuropsychological data and drafting/revising the manuscript. MF contributed to study concept, drafting/revising the manuscript and data verification. MAR contributed to study concept, patient recruitment, drafting/revising the manuscript, obtaining funding and data verification, acting as study supervisor. All the authors gave their approval to the current version of the manuscript.

Funding The study received no funding.

Declarations

Conflicts of interest R. Bonacchi, E. Pagani, and O. Marchesi have nothing to disclose. A. Meani received speaker honoraria from Biogen Idec. M. Filippi is Editor-in-Chief of the *Journal of Neurology* and Associate Editor of *Human Brain Mapping*, *Neurological Sciences*, and *Radiology*; received compensation for consulting services and/or speaking activities from Almiral, Alexion, Bayer, Biogen, Celgene, Eli Lilly, Genzyme, Merck-Serono, Novartis, Roche, Sanofi, Takeda, and Teva Pharmaceutical Industries; and receives research support from Biogen Idec, Merck-Serono, Novartis, Roche, Teva Pharmaceutical Industries, Italian Ministry of Health, Fondazione Italiana Sclerosi Multipla, and ARiSLA (Fondazione Italiana di Ricerca per la SLA). M.A. Rocca received speaker honoraria from Bayer, Biogen, Bristol Myers Squibb, Celgene, Genzyme, Merck Serono, Novartis, Roche, and Teva, and receives research support from the MS Society of Canada and Fondazione Italiana Sclerosi Multipla.

References

1. Altmann A, Tolosi L, Sander O, Lengauer T (2010) Permutation importance: a corrected feature importance measure. Bioinformatics 26:1340–1347
2. Anderson VM, Fisniku LK, Altmann DR, Thompson AJ, Miller DH (2009) MRI measures show significant cerebellar gray matter volume loss in multiple sclerosis and are associated with cerebellar dysfunction. Mult Scler 15:811–817
3. Anderson VM, Wheeler-Kingshott CA, Abdel-Aziz K, Miller DH, Toosy A, Thompson AJ, Ciccarelli O (2011) A comprehensive assessment of cerebellar damage in multiple sclerosis using diffusion tractography and volumetric analysis. Mult Scler 17:1079–1087
4. Benedict RH, Ramasamy D, Munschauer F, Weinstock-Guttman B, Zivadinov R (2009) Memory impairment in multiple sclerosis: correlation with deep grey matter and mesial temporal atrophy. J Neurol Neurosurg Psychiatry 80:201–206
5. Benjamini Y, Hochberg Y (1995) Controlling the false discovery rate: a practical and powerful approach to multiple testing. J Roy Stat Soc: Ser B (Methodol) 57:289–300
6. Bonacchi R, Pagani E, Meani A, Cacciaguerra L, Preziosa P, De Meo E, Filippi M, Rocca MA (2020) Clinical relevance of multiparametric MRI assessment of cervical cord damage in multiple sclerosis. Radiology 296:605–615
7. Calabrese M, Mattisi I, Rinaldi F, Favaretto A, Atzori M, Bernardi V, Barachino L, Romualdi C, Rinaldi L, Perini P, Gallo P (2010) Magnetic resonance evidence of cerebellar cortical pathology in multiple sclerosis. J Neurol Neurosurg Psychiatry 81:401–404
8. Cattaneo D, Gervasoni E, Anastasi D, Giovanni RD, Brichetto G, Carpinella I, Cavalla P, Confalonieri P, Groppo E, Prosperini L, Tacchino A, Rovaris M, Solaro C (2021) Prevalence and patterns of subclinical motor and cognitive impairments in non-disabled individuals with early multiple sclerosis: a multicenter cross-sectional study. Ann Phys Rehabil Med 65:101491
9. Charrad M, Ghazzali N, Boiteau V, Niknafs A (2014) NbClust: an R package for determining the relevant number of clusters in a data set. J Stat Soft 61:1–36
10. Cirillo S, Rocca MA, Ghezzi A, Valsasina P, Moiola L, Veggiotti P, Amato MP, Comi G, Falini A, Filippi M (2016) Abnormal cerebellar functional MRI connectivity in patients with paediatric multiple sclerosis. Mult Scler 22:292–301
11. Cocozza S, Petracca M, Mormina E, Buyukturkoglu K, Podranski K, Heinig MM, Pontillo G, Russo C, Tedeschi E, Russo CV, Costabile T, Lanzillo R, Harel A, Klineova S, Miller A, Brunetti A, Morra VB, Lublin F, Inglese M (2017) Cerebellar lobule atrophy and disability in progressive MS. J Neurol Neurosurg Psychiatry 88:1065–1072
12. Correale J, Gaitan MI, Ysrraelit MC, Fiol MP (2017) Progressive multiple sclerosis: from pathogenic mechanisms to treatment. Brain 140:527–546
13. D'Ambrosio A, Pagani E, Riccitelli GC, Colombo B, Rodegher M, Falini A, Comi G, Filippi M, Rocca MA (2017) Cerebellar contribution to motor and cognitive performance in multiple sclerosis: an MRI sub-regional volumetric analysis. Mult Scler 23:1194–1203
14. De Meo E, Portaccio E, Giorgio A, Ruano L, Goretti B, Niccolai C, Patti F, Chisari CG, Gallo P, Grossi P, Ghezzi A, Roscio M, Mattioli F, Stampatori C, Simone M, Viterbo RG, Bonacchi R, Rocca MA, De Stefano N, Filippi M, Amato MP (2021) Identifying the Distinct Cognitive Phenotypes in Multiple Sclerosis. JAMA Neurol 78:414–425
15. De Meo E, Storelli L, Moiola L, Ghezzi A, Veggiotti P, Filippi M, Rocca MA (2020) In vivo gradients of thalamic damage in

paediatric multiple sclerosis: a window into pathology. Brain 144:186–197
16. Diedrichsen J (2006) A spatially unbiased atlas template of the human cerebellum. Neuroimage 33:127–138
17. Eshaghi A, Marinescu RV, Young AL, Firth NC, Prados F, Jorge Cardoso M, Tur C, De Angelis F, Cawley N, Brownlee WJ, De Stefano N, Laura Stromillo M, Battaglini M, Ruggieri S, Gasperini C, Filippi M, Rocca MA, Rovira A, Sastre-Garriga J, Geurts JJG, Vrenken H, Wottschel V, Leurs CE, Uitdehaag B, Pirpamer L, Enzinger C, Ourselin S, Gandini Wheeler-Kingshott CA, Chard D, Thompson AJ, Barkhof F, Alexander DC, Ciccarelli O (2018) Progression of regional grey matter atrophy in multiple sclerosis. Brain 141:1665–1677
18. Eshaghi A, Young AL, Wijeratne PA, Prados F, Arnold DL, Narayanan S, Guttmann CRG, Barkhof F, Alexander DC, Thompson AJ, Chard D, Ciccarelli O (2021) Identifying multiple sclerosis subtypes using unsupervised machine learning and MRI data. Nat Commun 12:2078
19. Filippi M, Bruck W, Chard D, Fazekas F, Geurts JJG, Enzinger C, Hametner S, Kuhlmann T, Preziosa P, Rovira A, Schmierer K, Stadelmann C, Rocca MA, Attendees of the Correlation between P, workshop MRIfiM (2019) Association between pathological and MRI findings in multiple sclerosis. Lancet Neurol 18:198–210
20. Geurts JJ, Calabrese M, Fisher E, Rudick RA (2012) Measurement and clinical effect of grey matter pathology in multiple sclerosis. Lancet Neurol 11:1082–1092
21. Kutzelnigg A, Faber-Rod JC, Bauer J, Lucchinetti CF, Sorensen PS, Laursen H, Stadelmann C, Bruck W, Rauschka H, Schmidbauer M, Lassmann H (2007) Widespread demyelination in the cerebellar cortex in multiple sclerosis. Brain Pathol 17:38–44
22. Le M, Malpas C, Sharmin S, Horakova D, Havrdova E, Trojano M, Izquierdo G, Eichau S, Ozakbas S, Lugaresi A, Prat A, Girard M, Duquette P, Larochelle C, Alroughani R, Bergamaschi R, Sola P, Ferraro D, Grammond P, Grand' Maison F, Terzi M, Boz C, Hupperts R, Butzkueven H, Pucci E, Granella F, Van Pesch V, Soysal A, Yamout BI, Lechner-Scott J, Spitaleri D, Ampapa R, Turkoglu R, Iuliano G, Ramo-Tello C, Sanchez-Menoyo JL, Sidhom Y, Gouider R, Shaygannejad V, Prevost J, Altintas A, Fragoso YD, McCombe PA, Petersen T, Slee M, Barnett MH, Vucic S, Van Der Walt A, Kalincik T (2021) Disability outcomes of early cerebellar and brainstem symptoms in multiple sclerosis. Mult Scler J 27:755–766
23. Lublin FD, Reingold SC, Cohen JA, Cutter GR, Sorensen PS, Thompson AJ, Wolinsky JS, Balcer LJ, Banwell B, Barkhof F, Bebo B Jr, Calabresi PA, Clanet M, Comi G, Fox RJ, Freedman MS, Goodman AD, Inglese M, Kappos L, Kieseier BC, Lincoln JA, Lubetzki C, Miller AE, Montalban X, O'Connor PW, Petkau J, Pozzilli C, Rudick RA, Sormani MP, Stuve O, Waubant E, Polman CH (2014) Defining the clinical course of multiple sclerosis: the 2013 revisions. Neurology 83:278–286
24. Meijer KA, Steenwijk MD, Douw L, Schoonheim MM, Geurts JJG (2020) Long-range connections are more severely damaged and relevant for cognition in multiple sclerosis. Brain 143:150–160
25. Minagar A, Barnett MH, Benedict RH, Pelletier D, Pirko I, Sahraian MA, Frohman E, Zivadinov R (2013) The thalamus and multiple sclerosis: modern views on pathologic, imaging, and clinical aspects. Neurology 80:210–219
26. Moroso A, Ruet A, Lamargue-Hamel D, Munsch F, Deloire M, Coupe P, Ouallet JC, Planche V, Moscufo N, Meier DS, Tourdias T, Guttmann CR, Dousset V, Brochet B (2017) Posterior lobules of the cerebellum and information processing speed at various stages of multiple sclerosis. J Neurol Neurosurg Psychiatry 88:146–151
27. Parmar K, Stadelmann C, Rocca MA, Langdon D, D'Angelo E, D'Souza M, Burggraaff J, Wegner C, Sastre-Garriga J, Barrantes-Freer A, Dorn J, Uitdehaag BMJ, Montalban X, Wuerfel J, Enzinger C, Rovira A, Tintore M, Filippi M, Kappos L, Sprenger T, group Ms (2018) The role of the cerebellum in multiple sclerosis-150 years after Charcot. Neurosci Biobehav Rev 89:85–98
28. Patenaude B, Smith SM, Kennedy DN, Jenkinson M (2011) A Bayesian model of shape and appearance for subcortical brain segmentation. Neuroimage 56:907–922
29. Pietroboni AM, Schiano di Cola F, Colombi A, Carandini T, Fenoglio C, Ghezzi L, De Riz MA, Triulzi F, Scarpini E, Padovani A, Galimberti D (2020) CSF beta-amyloid predicts early cerebellar atrophy and is associated with a poor prognosis in multiple sclerosis. Mult Scler Relat Disord 37:101462
30. Preziosa P, Rocca MA, Mesaros S, Pagani E, Drulovic J, Stosic-Opincal T, Dackovic J, Copetti M, Caputo D, Filippi M (2014) Relationship between damage to the cerebellar peduncles and clinical disability in multiple sclerosis. Radiology 271:822–830
31. Rao SM, Leo GJ, Bernardin L, Unverzagt F (1991) Cognitive dysfunction in multiple sclerosis. I. Frequency, patterns, and prediction. Neurology 41:685–691
32. Rocca MA, Amato MP, De Stefano N, Enzinger C, Geurts JJ, Penner IK, Rovira A, Sumowski JF, Valsasina P, Filippi M, Group MS (2015) Clinical and imaging assessment of cognitive dysfunction in multiple sclerosis. Lancet Neurol 14:302–317
33. Rocca MA, Battaglini M, Benedict RH, De Stefano N, Geurts JJ, Henry RG, Horsfield MA, Jenkinson M, Pagani E, Filippi M (2017) Brain MRI atrophy quantification in MS: from methods to clinical application. Neurology 88:403–413
34. Rocca MA, Meani A, Fumagalli S, Pagani E, Gatti R, Martinelli-Boneschi F, Esposito F, Preziosa P, Cordani C, Comi G, Filippi M (2019) Functional and structural plasticity following action observation training in multiple sclerosis. Mult Scler 25:1472–1487
35. Rocca MA, Pagani E, Absinta M, Valsasina P, Falini A, Scotti G, Comi G, Filippi M (2007) Altered functional and structural connectivities in patients with MS: a 3-T study. Neurology 69:2136–2145
36. Schlaeger R, Papinutto N, Panara V, Bevan C, Lobach IV, Bucci M, Caverzasi E, Gelfand JM, Green AJ, Jordan KM, Stern WA, von Budingen HC, Waubant E, Zhu AH, Goodin DS, Cree BA, Hauser SL, Henry RG (2014) Spinal cord gray matter atrophy correlates with multiple sclerosis disability. Ann Neurol 76:568–580
37. Stoodley CJ, Schmahmann JD (2018) Functional topography of the human cerebellum. Handb Clin Neurol 154:59–70
38. Stoodley CJ, Valera EM, Schmahmann JD (2010) An fMRI study of intra-individual functional topography in the human cerebellum. Behav Neurol 23:65–79
39. Thompson AJ, Banwell BL, Barkhof F, Carroll WM, Coetzee T, Comi G, Correale J, Fazekas F, Filippi M, Freedman MS, Fujihara K, Galetta SL, Hartung HP, Kappos L, Lublin FD, Marrie RA, Miller AE, Miller DH, Montalban X, Mowry EM, Sorensen PS, Tintore M, Traboulsee AL, Trojano M, Uitdehaag BMJ, Vukusic S, Waubant E, Weinshenker BG, Reingold SC, Cohen JA (2018) Diagnosis of multiple sclerosis: 2017 revisions of the McDonald criteria. Lancet Neurol 17:162–173
40. Tsagkas C, Parmar K, Pezold S, Barro C, Chakravarty MM, Gaetano L, Naegelin Y, Amann M, Papadopoulou A, Wuerfel J, Kappos L, Kuhle J, Sprenger T, Granziera C, Magon S (2021) Classification of multiple sclerosis based on patterns of CNS regional atrophy covariance. Hum Brain Mapp 42:2399–2415
41. Valverde S, Cabezas M, Roura E, Gonzalez-Villa S, Pareto D, Vilanova JC, Ramio-Torrenta L, Rovira A, Oliver A, Llado X (2017) Improving automated multiple sclerosis lesion segmentation with a cascaded 3D convolutional neural network approach. Neuroimage 155:159–168
42. Valverde S, Oliver A, Llado X (2014) A white matter lesion-filling approach to improve brain tissue volume measurements. Neuroimage Clin 6:86–92

43. Van Overwalle F, Manto M, Cattaneo Z, Clausi S, Ferrari C, Gabrieli JDE, Guell X, Heleven E, Lupo M, Ma Q, Michelutti M, Olivito G, Pu M, Rice LC, Schmahmann JD, Siciliano L, Sokolov AA, Stoodley CJ, van Dun K, Vandervert L, Leggio M (2020) Consensus paper: cerebellum and social cognition. Cerebellum 19:833–868

44. Weier K, Banwell B, Cerasa A, Collins DL, Dogonowski AM, Lassmann H, Quattrone A, Sahraian MA, Siebner HR, Sprenger T (2015) The role of the cerebellum in multiple sclerosis. Cerebellum 14:364–374